ENGINEER - Vol. LIX, No. 02, pp. [135- 144], 2026

DOI: https://doi.org/10.4038/engineer.v59i2.7754

Development of Robust Controller for One Degree of Freedom Quasi-Zero Power Magnetically Suspended Thrust Bearing System

A.W.B.I. Annasiwaththa, S.M.S. Dinendra, P.M. Muthukumarana, I.P.R.R. Ilangarathna and H.E.T.S. Hewawasam

Abstract: Thrust bearings are often used in different industrial applications with varying axial loads. Despite such use, these conventional thrust bearings are incorporated with unclean operating environments and undergo wear and tear due to physical contact, making it challenging to use in controlled industrial environments where environmental cleanliness is a pivotal factor. This study presents the development of one degree of freedom magnetic suspension system equivalent to a vertical thrust bearing using a robust controller with a hybrid electromagnet which can perform disturbance rejection and handle model uncertainties. A finite element analysis has been performed to identify the properties of the hybrid electromagnet under varying parameters. The electrical system has been modelled as a RL circuit while a computer aided design of the mechanical system has been developed to analyse and validate the performance prior to the implementation in real system. The H_∞ robust controller has been developed using the mathematical model of the system, which was developed along with system analysis. The developed controller was validated under known external disturbances and model variations and the system behaviour was analysed. The results demonstrate that the developed H_∞ based system exhibits superior disturbance rejection compared to PID based control.

Keywords: Active Magnetic Bearing, Hybrid Magnetic Suspension, Magnetic Levitation, Quasi-Zero Power H_∞ Control

1. Introduction

Historically, thrust bearings have played a crucial role in mechanical engineering applications due to their ability to handle varying axial loads. Despite their excellent ability, these conventional thrust bearings are incorporated with unclean operating environments due to the use of lubricants such as oil and grease, dust particles and metal particles released due to physical contacts. Furthermore, the tolerances of the system change overtime due to wear and tear resulting from metal-to-metal contact within the components. Considering all these factors, use of conventional thrust bearings in industries such as semiconductor fabrication and medical industries under controlled environments have become a serious challenge where environmental cleanliness and accuracy are pivotal factors.

Magnetic bearings present possible alternative to conventional bearings with added complexity. But also with benefits such as clean operating environment, better precision control and noise and vibration isolation capability. Furthermore, magnetic thrust bearings possess the ability to damp the mechanical and electrical noise improving the system performance. Several studies have been carried out using simple control techniques such as PID controllers to stabilize such systems. Although they can operate under optimal conditions, they present limited ability to withstand system uncertainties and external disturbances which could occur when operating in real world systems. Therefore, the need of a contactless vertical thrust bearing system with a robust controller which can perform robust disturbance rejection is a timely concern. In this study, a robust controller which can perform above tasks

***Eng. (Dr.) A.W.B.I. Annasiwaththa**, AMIE(SL), PhD (KUT, Japan), MSc (Moratuwa, SL), B. Sc. Eng. (Moratuwa, SL), Senior Lecturer, Department of Mechanical and Manufacturing Engineering, University of Ruhuna, Sri Lanka.*
Email: annasi@mme.ruh.ac.lk
https://orcid.org/0009-0007-6267-3437
***Mr. S.M.S. Dinendra,** B. Sc. Eng. (Ruhuna, SL), Department of Mechanical and Manufacturing Engineering, University of Ruhuna, Sri Lanka.*
https://orcid.org/0009-0006-7131-2505
***Mr. P.M. Muthukumarana,** B. Sc. Eng. (Ruhuna, SL), Department of Mechanical and Manufacturing Engineering, University of Ruhuna, Sri Lanka.*
***Ms. I.P.R.R. Ilangarathna,** B. Sc. Eng. (Ruhuna, SL), Department of Mechanical and Manufacturing Engineering, University of Ruhuna, Sri Lanka.*
***Mr. H.E.T.S. Hewawasam,** B. Sc. Eng. (Ruhuna, SL), Department of Mechanical and Manufacturing Engineering, University of Ruhuna, Sri Lanka.*

has been developed for a one degree of freedom (DoF) magnetic suspension system equivalent to a vertical thrust bearing. A hybrid electromagnet has been used instead of a conventional bearing, eliminating the metal-to-metal contact between the shaft and the bearings, such that, the system does not require any lubrication and does not undergo wear and tear making it suitable for above mentioned applications. The hybrid electromagnet (HEM) consists of a permanent ring magnet and an electromagnet around it. The primary suspension force has been generated by the permanent ring magnet while it has been controlled using an integrated electromagnet. With reference to Figure 1, a shaft with a plate attached at the end goes through the ring magnet without any contact. The shaft and the shaft plate have been magnetically suspended, while maintaining a constant air gap. The system has been running as a closed loop control system where the air gap distance and the current flow in the electromagnet have been the system feedbacks. Using the developed robust controller, this study has successfully been able to drive the vertical thrust bearing system to Quazi-zero power state during the steady state operation under external disturbances and model parameter variations. Furthermore, the study provides a comparative analysis on system performance with baseline PID based control under the same operating conditions. The presented Quazi-zero power approach can achieve magnetic suspension while consuming near zero power system operation.

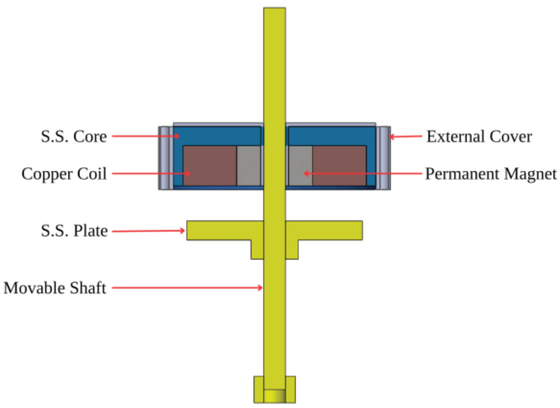

Figure 1 - Cross Section of the HEM

2. Literature Review

Magnetic suspension or levitation is a novel technology which has been applied in various industrial fields such as air compressors, transportation, small-scale and large-scale wind turbines and military weapons, aero-space, semiconductor fabrication and bio medical applications. Even though different kinds of approaches such as low temperature environments and super conductive elements have been used for those developments, use of zero power method to magnetically levitate the shaft plate requires continuous support from permanent magnets and electromagnets to counter gravitational force and external disturbances respectively [1]. Furthermore, magnetic levitation has been used for non-contact power transfer. It eliminates the difficulties of changing the batteries which has been a common challenge for levitated systems. The design consisted of 4 HEMs for levitation and linear motor for propulsion with an open-end generator [2]. The primary force was generated by the permanent magnet while voltage of the electromagnetic coil has been actively controlled to manipulate the electromagnetic force as required. The force generated by a HEM can be represented as in equation 1 where i is the coil current, z is the air gap distance between the plate and the magnet, and a, b and c are the constants unique to each system which needs to be determined via FEM analysis of electromagnetic system [3].

$$F = a\,(i + b)^2 / (z + c)^2 \qquad \dots (1)$$

2.1 Sensor Modelling and Noise Filtering

Probabilistic models for fault detection and identification are considered as some of the approaches to address sensor degradation [4].

Noise is often modelled using probabilistic sensor modelling methods with Gaussian distributions and Kernal density analysis techniques due to their widespread occurance. A standard approach to model sensor behaviour is through experiment data collection, where the sensor output is recorded for a known set of input values. This data set is then used to construct a probability density function which describes measurement uncertainty. Furthermore, the variability calculated under the sensor modelling could be directly used to define the process noise variance of the system.

Sensor measurements naturally contain noise due to various factors including electronic fluctuations, wire connection faults, environmental conditions and also with the hardware limitations [5].

Studies have proposed different noise filtering methods. Accoridng to [6], low pass filter provides noise attenuating at higher frequencies. It is simple and easier to implement. But it also introduces phase shifts which could affect the real time performance of the system. The author [6] also mentions about the moving average filter for noise reduction. However it cannot distinguish between noise and the actual signal leading to loss of information under rapid changes in smaller sample rate, making Kalman filter the most suitable method for a magnetic thrust bearing system. As previously mentioned, the process noise variation of the system has been directly utilized in the Kalman filter in this study while empirically tuning the measurement noise variance parameter to ensure balance between jitter and lag of the filter output.

2.2 Control Strategies for Magnetic Suspension

There are different types of control strategies that can be implemented as several studies have shown, according to the nature of the system itself and the behaviour expected. For example, [7] discussed vast amount research work done on Active Magnetic Bearings (AMB). From baseline controls such as PID to advanced modern control such as neural networks and fuzzy control have been used. The authors had highlighted the progress of different control strategies on AMBs. Although numerous examples have been reviewed, no work was found related to a vertical thrust bearing with robust control for disturbance rejection under quasi-zero power. The closest work had been the µ-synthesis control on a turbomolecular pump. Moreover, a study that has been done using PID control on flexible rotor dynamic magnetic bearing system with non-linear stiffness properties has revealed that linear control methods such as PID control might lead to vibrations with large amplitudes and potential loss of rotor dynamic stability [8]. Recently, a study has been done by [9], on detailed modelling and robust control of a multi-axis active magnetic bearing system. The authors had utilized optimal control methods such as Linear Quadratic Gaussian (LQG) to control the system. The results had shown better performance than the benchmark PID based controllers. However, the system does not involve a vertical thrust bearing with robust control method.

Meanwhile, several past studies have shown excellent outcomes using robust control approaches such as H_∞ control, H_2 control and μ synthesis method. According to [10], H_2 control method minimizes the effect of disturbances on the system by reducing the overall energy of the system's response. The authors have further stated that H_2 control is best designed for well-defined disturbances and therefore it is not inherently robust against model uncertainties. As a result, it might not provide best performance under unpredictable changes.

Another study has shown the application of both H_∞ and H_2 control methods on magnetic bearings in horizontal rotating machinery. The study has also extended to use of PID control for further analysis. The results show that selecting the weighting functions for robust controllers is critical as it determines tracking and robustness trade off. The comparison between H_∞ and H_2 control has shown distinct results where H_∞ is better at handling worst case disturbance and ensuring robust stability, making it suitable for systems with significant uncertainties. In contrast, H_2 control method provides optimal performance, under typical operating conditions, focusing on minimizing the average impact of disturbances. A mixed H_∞-H_2 approach has been tested for a magnetic levitation actuator which is used in microgravity vibration isolation systems. The study has further addressed the trade-off between robust stability and nominal performance, demonstrating that the mixed controller effectively supressed acceleration vibrations and works better than traditional PIDs in attenuation of amplitude across various frequencies [11].

The μ synthesis method provides guaranteed robustness using its D-K iteration. But the performance is based on how well structured the disturbances are, and it is computationally intensive than previously mentioned robust control methods [10].

A comprehensive review of the existing literature reveals several critical insights into system optimization and robust control. Among various filtering techniques, the Kalman filter is identified as the most suitable method due to its high precision and predictive capabilities. Furthermore, while traditional PID control is widely used, it lacks the necessary resilience against high-range parameter variations. In contrast, the H_∞ control method demonstrates superior performance under unstructured disturbances, provided that weighting functions are carefully selected to balance robustness and performance. Despite these advancements in control and sensing, a significant research gap remains in the development of a quasi-zero power magnetically suspended vertical thrust bearing that effectively includes these techniques.

3. System Design

The system contains the mechanical design, development of the mathematical model, development of the virtual model and the development of the prototype system with hardware.

3.1 Mechanical Design of the System

The system consists of a HEM which includes a permanent ring magnet (Reversible N42) and an electro magnet developed utilizing copper wires of cross-sectional diameter 0.64 mm (AWG 22) in order to withstand a designed maximum current of 3.0 A. The HEM is embedded inside a ss400 core and the total assembly is covered with an aluminium shell. As shown by Figure 1, the shaft is going through the HEM and the shaft plate is fixed to the shaft providing a 1 DoF movement through vertical translation. Furthermore, the movable shaft does not make contact with the hybrid permanent magnet assembly. Therefore, the design eliminates the previously discussed limitations. The air gap distance is measured using Omron ZX-LD40 laser distance sensor. Figure 2 shows computer aided design (CAD) of the full assembly of the system along with the supportive structure for the HEM assembly and the distance sensor which is mounted at the bottom of the structure. Figure 3 shows the fabricated prototype system.

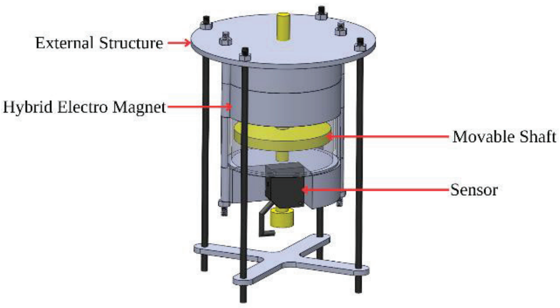

Figure 2 - Design of Full Assembly of the System

Figure 3 - Prototype System

3.2 Development of the Mathematical Model

Table 1 shows the system parameters and their respective values.

Table 1 - System Parameters

Symbol	Description	Value
m	Mass of the shaft and plate	0.762 kg
R	Coil Resistance	10.11 Ω
L	Coil Inductance	30.33 mH
Z_0	Zero Power Air Gap (Obtained via FEM modelling)	23.44 mm
a	Constants to define HEM Model	2.185e-5 Nm^2A^{-2}
b		-8.963 A
c		-8.02e-3m
$F(i, z)$	Magnetic Force of HEM	
v	Coil Voltage	
i	Coil Current	
z	Air Gap	

The complete system is segmented in to three main subsystems, namely, the magnetic system consisting the HEM, electrical system of the coil of the electromagnet and the mechanical system. The mathematical models of the three subsystems were separately developed and augmented into a single system to model the system as a single model describing dynamic behaviour of electromagnetic suspension system.

3.2.1 Model of the magnetic system

The force generated by the magnetic force can be represented using equation 1. Equation 2 shows the linearized model of HEM around the operating point of zero coil current (I_0) and Z_0 air gap.

$$F_{(linear)} = F_{(Z_0,I_0)} + k_i\delta i - k_z\delta z$$

$$[F_{(z,i)}]_{Z_0,I_0} = mg + k_i\delta I - k_z\delta Z \qquad \dots (2)$$

where,

$$k_i = 2ab/(Z_0 + c)^2$$

$$k_z = 2ab^2/(Z_0 + c)^3$$

To estimate the values of the a, b and c constants, finite element analysis (FEA) was performed on the HEM to identify relationship between airgap, coil current and electromagnetic force. The analysis contained the hybrid electromagnet and the shaft with shaft plate. After an iterative process to find the number of turns needed, the selected coil consisted of 1000 turns. Coil current varied from -3 A to 3 A with 0.25 A increment. The shaft and the shaft plate were moved along its axis away from the magnet in 0.1 mm increments. Figure 4 shows how the obtained data are surface fitted with a RMSE value of 0.0273 N for the equation 1 discussed earlier, in order to calculate the constant values *a*, *b* and *c* describing the HEM model. The dots of Figure 4 show the data points obtained via FEA.

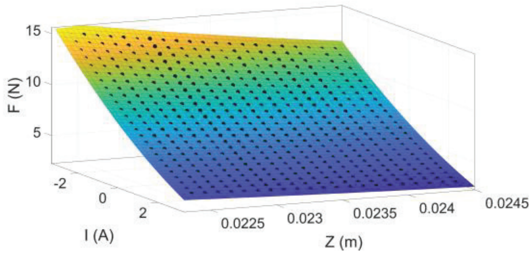

Figure 4 - HEM Force vs. Air Gap and Current

3.2.2 Model of the electrical system

The electrical circuit is modelled as a series RL circuit which is the coil of the electromagnet as shown in equation 3. The input to the system is the voltage while current flow is measured as the output.

$$V = IR + L(dI/dt) \quad \dots (3)$$

$$dI/dt = -(R/L)\, I + (1/L)V$$

3.2.3 State space model of the complete system

The complete state space model of the system can be derived by augmenting the previously derived models with the model of the mechanical system by applying Newtonian equation of motion. The state space model of the system can be represented as in equation 4 for the considered states.

$$\begin{bmatrix} \dot{z} \\ \ddot{z} \\ \dot{I} \end{bmatrix} = \begin{bmatrix} 0 & 1 & 0 \\ {k_z}/{m} & 0 & {-k_i}/{m} \\ 0 & 0 & {-R}/{L} \end{bmatrix} \begin{bmatrix} z \\ \dot{z} \\ I \end{bmatrix} + \begin{bmatrix} 0 \\ 0 \\ {1}/{L} \end{bmatrix} V \quad \dots (4)$$

3.3 Design of the Robust Controller

Considering the uncertainties and the external disturbances that could occur in the real-world applications, and the purposes of different robust control methods, H_∞ controller was designed for the system. The H_∞ controller was designed such that; it rejects disturbances at high frequencies and compensate model uncertainties by minimizing the H_∞ norm of the system which is shown by equation 5.

$$||F_{(j\omega)}||_{\omega} = sup_{\omega}\, \sigma_{max}\, F_{(j\omega)} \quad \dots (5)$$

where,

sup_{ω} = *Supremum of all the frequencies*

σ_{max} = *Maximum sigular value*

$F_{(j\omega)}$ = *Frequency domain transfer function*

The nominal plant model, which has been derived previously, was augmented with the weighting functions W_S, W_U and W_T respectively. W_S is defined for capturing the level of disturbance rejection or performance while W_T is defined for enforcing robustness. Wu is defined for penalizing the system input. During this study, *Wu* has been kept at unity which allows the controller to achieve robustness at any input without penalizing. Equations 6 and 7 show the defined weighting functions.

$$W_S = M\omega_c/(s + \omega_c) \quad \dots (6)$$

$$W_T = s\omega_c/(As + \omega_c) \quad \dots (7)$$

where,

M = *Low frequency gain of* W_S
ω_c = *Cut-off Frequency (1/3 to 1/10 of Natural Frequency)*

ω_c/A = *High Frequency gain of* W_T

In equations 6 and 7, W_S is defined as a low pass filter while W_T as a high pass filter. Therefore, they become dominant in low frequencies and high frequencies, complementary to each other. Moreover, they act as tuning parameters for the sensitivity and the complementary sensitivity of the control problem. It should be mentioned that this controller design has not designed for penalizing the system input, which means enforcing the robustness is the main priority at any input cost.
Once the weight functions are defined, the generalized plant model is developed by augmenting the nominal plant with the weight functions as shown below where *G* represents the nominal plant model and *P* represents the generalized augmented plant. Moreover, the weight functions are represented as respective state space models.

$$G = \begin{bmatrix} A & B \\ C & D \end{bmatrix} \quad \dots (8)$$

$$W_S = \begin{bmatrix} A_S & B_S \\ C_S & D_S \end{bmatrix} \quad \dots (9)$$

$$W_T = \begin{bmatrix} A_T & B_T \\ C_T & D_T \end{bmatrix} \quad \dots (10)$$

$$P = \begin{bmatrix} W_S & -W_sG \\ 0 & I \\ 0 & W_TG \\ I & -G \end{bmatrix} \quad \dots (11)$$

The generalized augmented plant shown in Figure 5 is used for developing the feedforward gain (*K*) for the closed loop system whereas, *u* is the control input, *v* is the measurable variables, *w* is the disturbance and *z* is the state error.

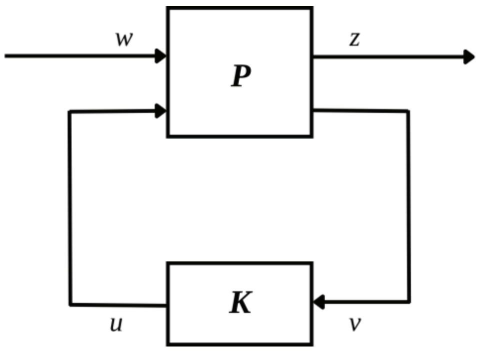

Figure 5 - Generalized Augmented Closed Loop System

The feedforward gain (*K*) is achieved by solving the Riccati equation minimizing the cost function (γ) of the augmented system ($\gamma = min||P||$) such that according to the minimum gain theory, the H_∞ norm should be less than unity.

After augmenting the nominal plant with the weight functions, the H_∞ gain was designed in MATLAB using the augmented plant as a feedforward gain. Equation 8 shows the designed high order dynamic H_∞ feedforward gain (*K*) according to the defined parameters and performance level.

$$K = \frac{2.3e14s^4+1.7e17s^3+3.3e19s^2+1.3e21s+9.4e21}{s^5+1.4e5s^4+6e9s^3+1.4e14s^2+2.0e16s+5.3e17} \quad \dots (12)$$

3.4 Development of the Virtual Model

To validate the performance of the deigned controller, a virtual model was developed using the CAD model which was designed previously. The sensor noise of the real sensor was modelled with a calculated variance of 7.48 x 10^{-10} m^2 using probabilistic sensor modelling to make the virtual system as much as close to the real-world conditions. Moreover, a Kalman filter was used to filter high frequency noise from air gap measurement.

The control architecture was developed inside the virtual system as a closed loop feedback system. In addition to the H_∞ controller, a discrete I controller has been used to drive the system to the zero-power state.

Figure 6 shows the control architecture of the virtual model.

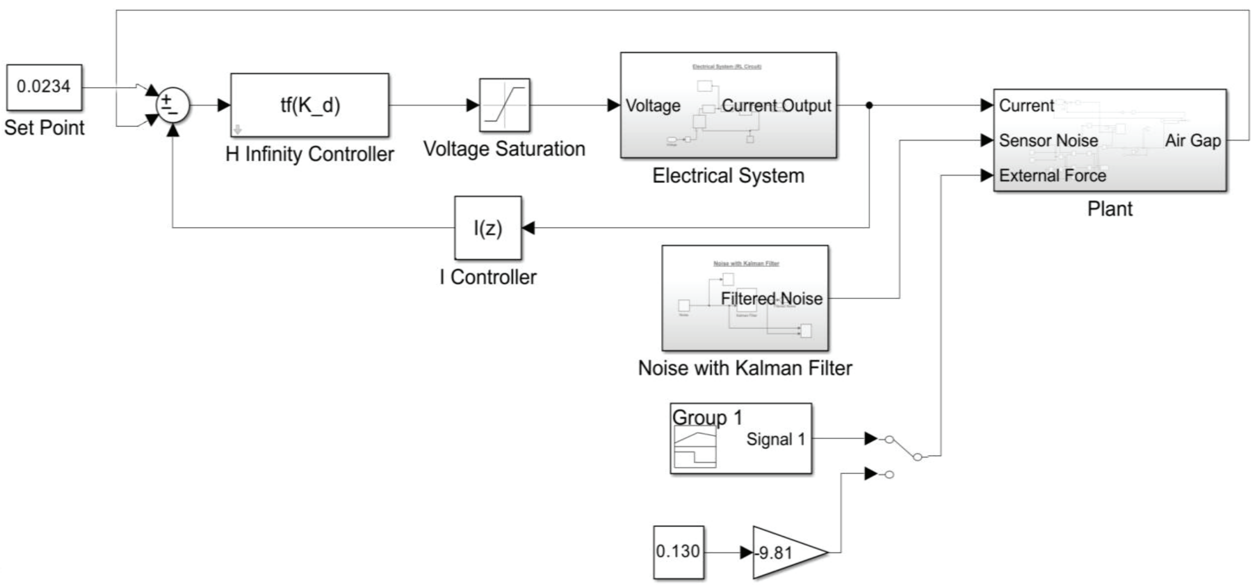

Figure 7 shows the virtual model of the electrical system which was a Resistor-Inductor (RL) circuit. The Electrical system represents the coil of the electromagnet.

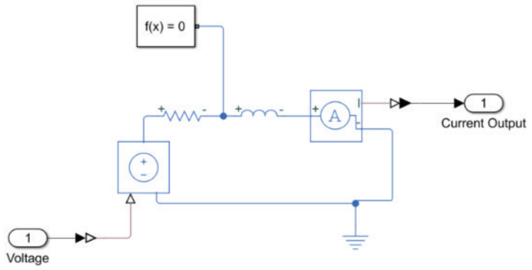

Figure 7 - Model of the Electrical System

In addition to the above controller, a simple controller using discrete PD and an I controller was developed to build a comparative analysis on the system behaviour under two control methods. The validated results using the virtual model is discussed in the section 4 of this paper.

3.5 Development of the Real Time Controller with Hardware

Once the developed controllers were validated in the virtual environment, the real time controller for the hardware set up was built. Figure 8 shows the real time closed loop system with both H_∞ and PID controllers.

4. Results and Discussion

The results contain the frequency domain analysis and the system behaviour comparison with both H_∞ and PID controllers in both virtual environment and real system.

4.1 Frequency Domain Analysis of H_∞ Controller

Since the H_∞ controller is a high order dynamic feedforward controller, the controller behaviour is varying with the frequency. In the design procedure also, the augmentation with weighting functions is based on attenuating the output with regard to the cut-off frequency specified. Therefore, it is important to analyse the performance of the controller in frequency domain.

Figure 9 shows the magnitude and phase bode of the nominal plant without any controller. The plot shows that the nominal plant model is unstable since it has a Gain Margin greater than 80dB and phase margin of infinity.

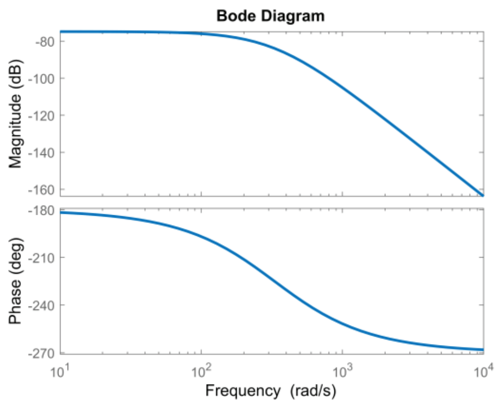

Figure 9 – Frequency Response of Nominal Plant

Figure 10 shows the singular value plot of the two weighing functions that have been used. As the figure shows, the two functions have provided the expected output action as a low

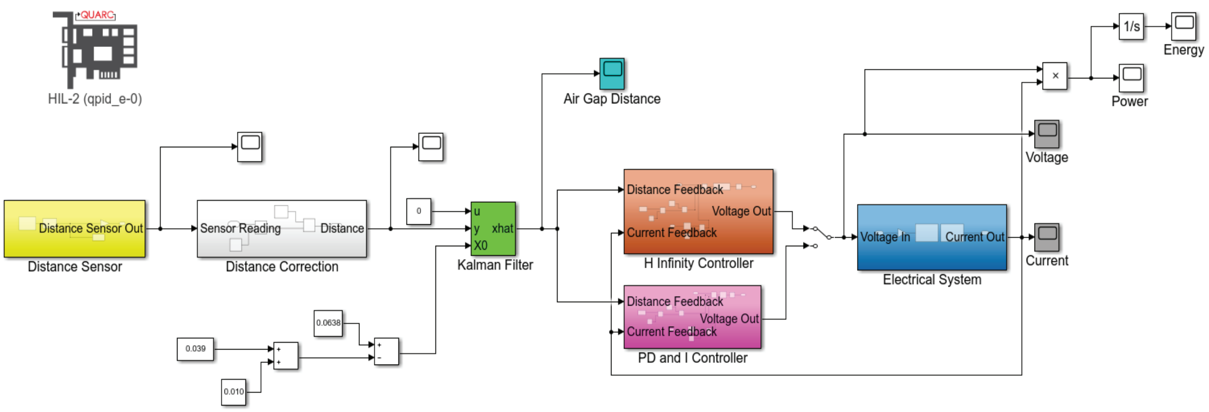

Figure 8 - Real Time Closed Loop System Implemented on Prototype

pass filter and a high pass filter. The high frequency gain of the system has been lower than the low frequency gain, which has been helpful to prevent disturbance amplification at higher frequencies. Furthermore, the figure shows that the weighing functions have avoided the system reaching its natural frequency (365 rad/s) so that oscillations do not occur.

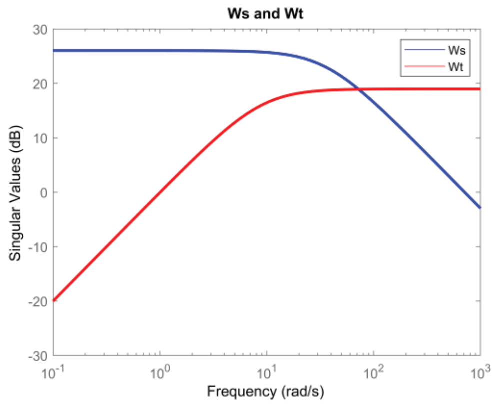

Figure 10 - Frequency Response of W_S and W_T

Figure 11 shows the comparison of the frequency response between the open loop nominal plant and the closed loop plant with the H_∞ controller. The Figure clearly shows how the controller has minimized the low frequency gain of the system and also the controller has been able to maintain it for frequencies up to 10^4 rad/s. The closed loop system has a gain margin of 2.12dB and a phase margin of 107.47 which proves the output in the Figure 10.

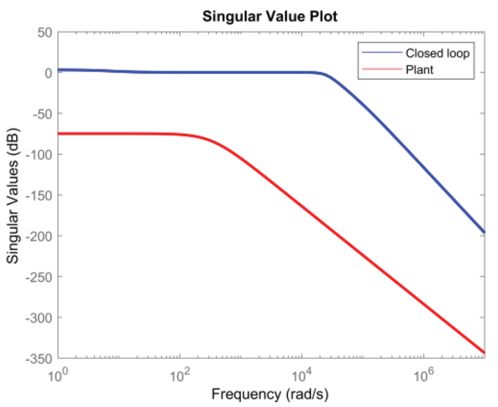

Figure 11 - Frequency Response of Open Loop Plant vs Closed Loop Plant

4.2 Virtual Model Results

Before implementing controllers with the real system, both the controllers; H_∞ controller and PID controller were validated within the virtual environment. The results showed the difference between the two controllers under the same conditions with sensor noise and external disturbances. The H_∞ controller has shown promising results with regards to its robustness.

Figure 12 shows how the H_∞ controller has minimized the system response compared to PID controller. The minor oscillations for H_∞ controller are characteristics of a robust controller.

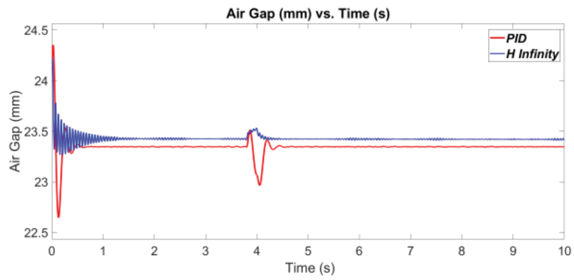

Figure 12 - Air Gap Variation under H inf. vs. PID in Virtual System

Figure 13 and Figure 14 show that both controllers have been able to achieve zero power state inside the virtual system. However, H_∞ controller has not allowed large overshoots like in PID.

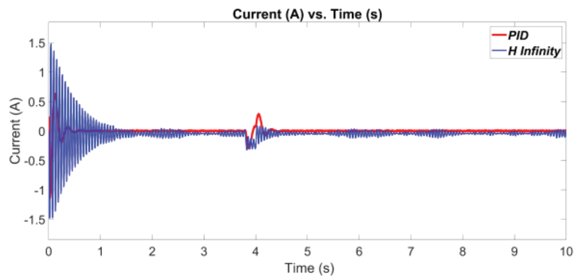

Figure 13 - Current Variation under *H* inf. vs. PID in Virtual System

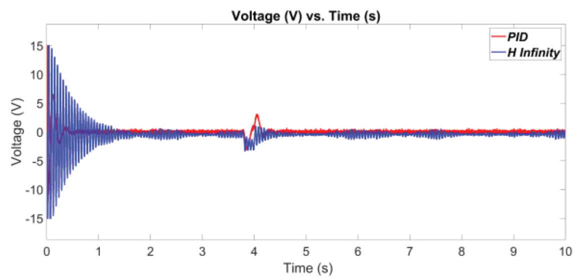

Figure 14 - Voltage Variation under *H* inf. vs. PID in Virtual System

The above results show that the performance of the designed H_∞ controller and the PID controller have reached an acceptable level. As the virtual system was modelled as much as close to real world conditions, the controllers were tested with the real system.

4.3 Prototype System Results

Using the prototype system, the designed controllers were tested for their performance. In order to validate the robustness of the H_∞ controller against external disturbances, the research team carried out a comparative analysis between the behaviour of H_∞ controlled system and the PID controlled system under two conditions. They are,

- Without external disturbances
- Under a step input force

4.3.1 Without external disturbances

Figure 15 and Figure 16 show how the current and the voltage has been varied without any external disturbances to the system. Both the behaviours under H_∞ controller and PID controller have been recorded under same initial conditions and environmental conditions. By analysing the Figures, it can be clearly observed that both controllers have been able to achieve the zero-power steady state. The most significant feature is the performance of the H_∞ controller. It has been able to achieve the tracking level of the PID controller while being robust.

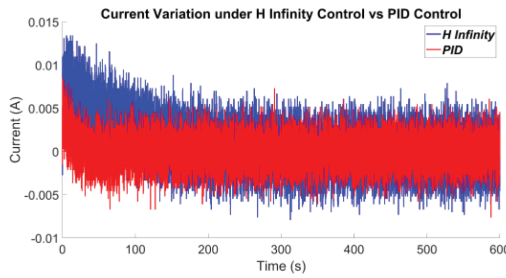

Figure 15 - Current Variation under *H* inf. vs. PID in Real System

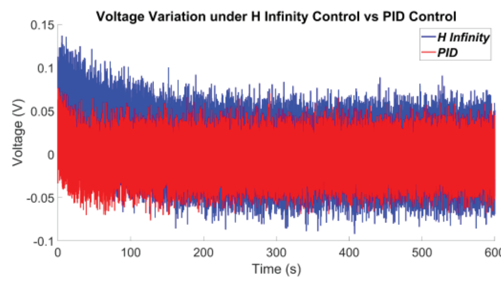

Figure 16 - Voltage Variation under *H* inf. vs. PID in Real System

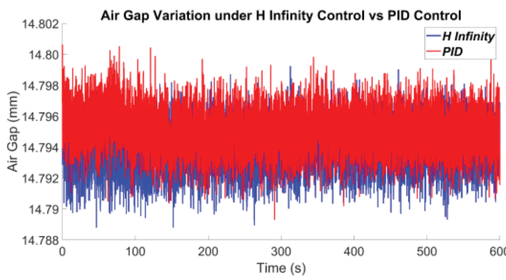

Figure 17 - Air Gap Variation under *H* inf. vs. PID in Real System

4.3.2 Under a step input force

With equal initial conditions and environmental conditions, the same system was given a step input force of 2 N at the top of the shaft at 300 s timestamp. After stabilizing at zero power state initially, with the step input given, Figure 18 to 20 show how the two systems have responded. PID controlled system has shown a higher response with a larger overshoot compared to H_∞ controlled system. But the PID controller has brought the system to steady state faster than the H_∞ controller proving its tracking ability. With a smaller overshoot the robust controller has brought the system to zero power steady state slowly. Table 2 shows the parameters of the variation of current under both controllers. The PID controlled system clearly shows a sudden peak when the thrust bearing gets an axial load.

Table 2 - Parameters of Current Variation under *H* inf vs. PID

	H_∞	PID
External Force	2 N	2 N
Peak Value	0.03 A	0.07 A

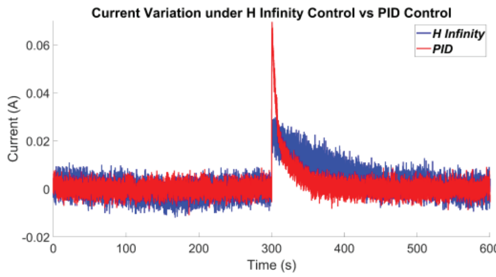

Figure 18 - Current Variation under *H* inf. vs. PID with Step Input Force in Real System

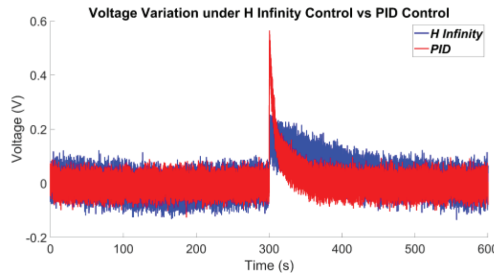

Figure 19 - Voltage Variation under *H* inf. vs. PID with Step Input Force in Real System

The air gap variation comparison in Figure 20 clearly shows the difference between the H_∞ controller and the PID controller. For an equal step input force, the air gap of PID controlled system has changed by nearly five times the change by H_∞ controlled system proving the disturbance rejection by the H_∞ controller. Furthermore, the results show how the H_∞ controller allows to use a low voltage supply compared to PID controller to achieve the steady state for the same system.

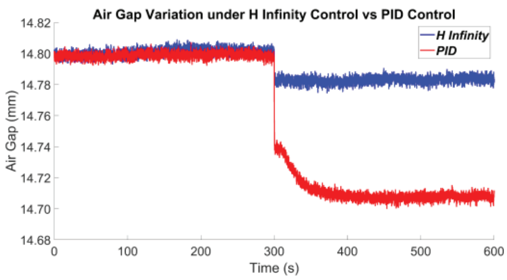

Figure 20 - Air Gap Variation under *H* inf. vs. PID with Step Input Force in Real System

5. Conclusion

This study has successfully been able the develop a robust controller for one degree of freedom Quazi-zero power magnetically suspended thrust bearing. Followed by the system design process, the system performance was validated in both virtual environment and the developed protype. The results show achieving Quazi-zero power state under external disturbances. When an external step load applied axially to the levitated thrust bearing, the PID controlled system has shown a significant airgap change response, nearly two times the peak response of H_∞ controlled system, highlighting the improved robustness of the magnetic thrust bearing. Furthermore, the results show how the robust control can be utilized with a lower power compared to the PID controlled system. The key contribution of this study is the development of disturbance resilient magnetic thrust bearing with advanced robust control. Development of a multiple degree of freedom magnetic thrust bearing with rotating shaft could be a valued future research direction for this study eliminating the main drawback of the current system; which has only 1 DoF vertical translation. Overall, this study provides a detailed analysis of an improved stability, energy efficient and disturbance resilient magnetically levitated thrust bearing system.

Acknowledgement

The research team expresses their sincere gratitude to the Faculty of Engineering of University of Ruhuna for providing its support and resources throughout this study.

References

1. Amirthakulasingam, G., Hewage, H. & Annasiwaththa, B., "Modelling and Simulation of 3 DOF Electromagnetic Levitated Platform with Zero-Power Control," in *2021 10th International Conference on Information and Automation for Sustainability (ICIAfS)*, Negambo, Sri Lanka, 2021.
2. Annasiwaththa, B. & Oka, K., "Design Concept and Analysis of a Magnetically Levitated Linear Slider with Non Contact Power Transfer," *International Journal of Applied Electromagnetics and Mechanics,* Vol. 52, No. 1-2, p. 207–213, 2016.
3. Annasiwaththa, B., Oka, K. & Harada, A., "Magnetically Levitated Linear Slider with a Non-Contact Power Transfer Method," *International Journal of Applied Electromagnetics and Mechanics,* Vol. 54, No. 2, pp. 223-237, 2017.
4. Hossain, R., Kobayashi, K. & Alam, S., "Sensor Degradation in Nuclear Reactor Pressure Vessels: The Overlooked Factor in Remaining Useful Life Prediction," 12 July 2024. [Online]. Available: https://www.nature.com/articles/s41529-024-00484-4. [Accessed 07 November 2025].
5. Wang, L. & Guan, R., State Feedback Control and Kalman Filtering, West Sussex: John Wiley & Sons Ltd, 2023.
6. Smith, G., "What is Signal Processing?," DEWESoft d.o.o., 14 March 2023. [Online]. Available: https://dewesoft.com/blog/what-is-signal-processing. [Accessed 07 November 2025].
7. Nehal, T., Hamanah, W.& Ali, M., "Advancements in Optimization Techniques for Active Magnetic Bearing Systems: Current Trends and Future Directions," *IEEE Access,* vol. 4, 2025.
8. Hongphan, T., Cole, M. & Brand, Z, "H-Infinity Controller Design for Efficiency Optimization of Magnetic Bearings in a Flywheel Energy Storage System," in *3rd International Conference on Energy and Power ICEP2021*, 2021.
9. Hassan, M., Ahad, M., Ali, Q. & Ishfaq, S., "Detailed Modeling and Robust Control of a Multi-Axis Active Magnetic Bearing System," *Journal of the Brazilian Society of Mechanical Sciences and Engineering,* Vol. 48, No. 217(2026), 2026.
10. Liu, K. & Yao, Y., Robust Control, Singapore: John Wiley & Sons (Asia) Pte Ltd, 2016.
11. Yalcin, B.& Erkan, K., "3-DoF Zero Power Micro Vibration Isolation via Linear Matrix Inequalities Based on H∞ and H2 Control Approaches," *Mechanical Systems and Signal Processing,* Vol. 153, 2021.